Performance Evaluation of an OFDM-Based Physical Layer for 5G LTE Wireless Networks

Ripudaman Chaturvedi[1], Sandeep Ojha[2], and Alok Kumar Mishra[3]
[1]*Department of Electronics and Communication Engineering, RITM, Lucknow*
[2]*Department of Electrical Engineering, RITM, Lucknow*
[3]*Department of Electronics and Communication Engineering, RITM, Lucknow*

Abstract— **The rapid advancements in modern communication systems demand robust, scalable wireless networks. This paper investigates the design and performance analysis of a 5G LTE physical layer based on Orthogonal Frequency Division Multiplexing (OFDM). A simulation model is developed in MATLAB/Simulink to evaluate Bit Error Rate (BER) performance under Additive White Gaussian Noise (AWGN) and multipath Rayleigh fading channels. Advanced modulation schemes such as BPSK, QPSK, and QAM are implemented with adaptive decision control to improve spectral efficiency. The study demonstrates that effective channel estimation and adaptive modulation significantly enhance system reliability in dynamic wireless environments. These results contribute to the development of practical high-speed broadband access, particularly for urban and rural applications where traditional wired infrastructure is not feasible.**

Index Terms— 5G LTE, OFDM, Adaptive Modulation, Channel Estimation, MATLAB Simulation, Broadband Wireless Access

I. INTRODUCTION

In the current era of rapid digital transformation, the demand for high-speed, reliable, and ubiquitous broadband wireless access has surged dramatically. This demand is driven by the exponential growth in connected devices, the proliferation of multimedia services, and the increasing need for seamless mobility across urban and rural landscapes alike. Conventional wired infrastructure, such as DSL and cable, although highly reliable, often fails to reach geographically remote or economically challenging areas where the cost of deployment is prohibitive. To address this digital divide, wireless broadband access technologies have evolved significantly over the past two decades, with the IEEE 802.16 family of standards playing a pivotal role in shaping the landscape.

The IEEE 802.16 standard, commonly known as WiMAX (Worldwide Interoperability for Microwave Access), laid the groundwork for the development of robust wireless metropolitan area networks (Wireless MANs). Initially designed for fixed broadband wireless access (BWA) under Line-of-Sight (LOS) conditions in high-frequency licensed bands, the standard was progressively enhanced to accommodate Non-Line-of-Sight (NLOS) scenarios through amendments such as IEEE 802.16a and IEEE 802.16e. These enhancements introduced advanced features like Orthogonal Frequency Division Multiplexing (OFDM), Orthogonal Frequency Division Multiple Access (OFDMA), Multiple-Input Multiple-Output (MIMO) systems, and Adaptive Modulation and Coding (AMC). Together, these technologies significantly improved spectral efficiency, coverage, and overall system robustness.

The emergence of fifth-generation (5G) cellular networks represents the culmination of these technological advancements, extending the capabilities of broadband wireless access to unprecedented levels. 5G LTE, which builds upon the foundations laid by the IEEE 802.16e-2005 standard, aims to provide ultra-reliable, low-latency, high-throughput wireless connectivity across diverse application scenarios, ranging from dense urban environments to remote rural regions. The architecture of 5G LTE incorporates key innovations at the physical (PHY) and medium access control (MAC) layers, enabling dynamic adaptation to variable channel conditions, user mobility, and diverse Quality of Service (QoS) requirements.

One of the critical components underpinning the success of 5G LTE is the deployment of OFDM and OFDMA technologies. OFDM effectively partitions the available frequency spectrum into multiple orthogonal subcarriers, each carrying a portion of the data stream. This multicarrier approach not only mitigates Inter-Symbol Interference (ISI) caused by multipath fading but also enhances spectral efficiency by eliminating the need for large guard bands. Meanwhile, OFDMA extends the benefits of OFDM by enabling multiple users to share the spectrum simultaneously, assigning different subsets of subcarriers to each user based on real-time channel conditions and data rate requirements. This capability ensures efficient resource allocation and maximizes throughput, particularly in scenarios involving high user density and mobility.

Despite these advantages, implementing an OFDM-based physical layer for 5G LTE poses several challenges. One major challenge is the high Peak-to-Average Power Ratio (PAPR) inherent in OFDM signals, which complicates the design of power amplifiers that must handle significant amplitude fluctuations without introducing non-linear distortions. Furthermore, wireless channels are inherently susceptible to fading, shadowing, and Doppler shifts, especially in mobile environments. These factors necessitate robust channel estimation and equalization techniques to maintain reliable data transmission at acceptable Bit Error Rates (BER). The integration of adaptive modulation and coding schemes is therefore essential, enabling the system to dynamically adjust its transmission parameters in response to changing channel conditions and user requirements.

A considerable body of literature has addressed various aspects of these challenges, proposing innovative solutions to optimize resource allocation, enhance spectral efficiency, and improve system resilience. In [1] explored the use of Particle Swarm Optimization (PSO) for adaptive subchannel allocation in OFDMA systems. Their study demonstrated that a PSO-based approach could efficiently allocate subchannels by maximizing channel gains and employing a water-filling algorithm for power distribution. Compared to traditional allocation methods, the PSO algorithm achieved higher sum capacities with reduced computational complexity, making it well-suited for real-time applications in IEEE 802.16e-based networks.

In another significant contribution, [2] investigated the effects of incorporating wavelet transforms into MIMO-OFDM systems to combat the adverse impact of multipath fading. By combining OFDM, Code Division Multiple Access (CDMA), and a modified Space Shift Keying (SSK) technique, the study demonstrated notable improvements in BER performance, particularly in scenarios with severe Rayleigh fading. The proposed hybrid model leveraged frequency and time diversity while minimizing inter-antenna interference, underscoring the potential of advanced signal processing techniques in enhancing wireless link robustness.

In [3] conducted a comprehensive analysis of the impact of dynamic overhead on the performance of Mobile WiMAX systems, which serve as a precursor to modern 5G LTE networks. Their research emphasized the significance of accurately Modeling physical layer signalling overhead to ensure realistic performance evaluations. By introducing dynamic overhead models for both uplink and downlink channels, the study revealed that simulation results based on average overhead values closely approximate those obtained using fully dynamic calculations. This insight simplifies system-level design processes without compromising simulation fidelity.

Additionally, various researchers have examined the performance trade-offs associated with different modulation schemes in OFDM-based wireless systems. While higher-order modulation schemes like 16-QAM and 64-QAM offer increased data rates, they are more susceptible to noise and fading, making them less reliable in challenging channel conditions. Conversely, lower-order schemes such as BPSK and QPSK provide greater resilience at the expense of spectral efficiency. Adaptive modulation techniques play a vital role in balancing these trade-offs by dynamically selecting the optimal scheme based on real-time SNR measurements. This approach ensures that throughput and reliability are maximized simultaneously, regardless of fluctuations in channel quality.

The deployment of robust channel estimation and equalization methods is equally critical. Pilot-based channel estimation, for example, inserts known pilot symbols into the transmission, enabling the receiver to estimate and compensate for channel-induced distortions. This technique significantly improves BER performance, particularly in fading environments. Simulation studies conducted using MATLAB/Simulink platforms have demonstrated the practical effectiveness of these methods, providing valuable insights into real-world implementation scenarios.

Collectively, these studies highlight the ongoing evolution of broadband wireless access technologies and the crucial role of intelligent system design in realizing the full potential of 5G LTE networks. By addressing challenges such as multipath fading, high PAPR, and dynamic user mobility through advanced signal processing, adaptive modulation, and resource allocation algorithms, researchers continue to push the boundaries of wireless communication performance.

In this paper, we build upon these foundations by developing a comprehensive simulation model of an OFDM-based 5G LTE physical layer. The model is designed to evaluate BER performance under various channel conditions, including AWGN and multipath Rayleigh fading, while implementing adaptive modulation schemes and pilot-based channel estimation techniques. By analyzing the system's performance across different scenarios, this work aims to provide practical insights into the design considerations and trade-offs involved in deploying next-generation broadband wireless systems capable of meeting the diverse demands of modern digital communication.

The organization of this paper is as follows: After this introduction and literature review, Section 2 describes the detailed system model and simulation methodology, including the design of the OFDM physical layer and channel conditions considered. Section 3 presents and discusses the simulation results, highlighting key findings on BER performance under various scenarios. Section 4 concludes the paper by summarizing the contributions and outlining potential directions for future work.

II. SYSTEM MODEL AND METHODOLOGY

The system model in this study is designed to evaluate the performance of an OFDM-based physical layer for 5G LTE networks under realistic wireless channel conditions. This section describes the core components of the proposed simulation framework, the design assumptions, the key signal processing blocks, and the simulation parameters used to investigate the effects of noise, fading, and adaptive modulation on system performance.

Orthogonal Frequency Division Multiplexing (OFDM) is a multicarrier modulation technique that divides the available spectrum into multiple orthogonal subcarriers, each modulated by a low-rate data stream. This approach offers high spectral efficiency and robustness against frequency-selective fading and inter-symbol interference (ISI), making it particularly suitable for broadband wireless applications such as 5G LTE.

In the proposed system, the OFDM transmitter begins with input data generated by the Medium Access Control (MAC) layer. These data packets are randomized to eliminate long runs of zeros or ones, which improves the statistical properties of the transmitted signal and enhances error correction performance.

Next, the randomized data undergo channel coding using a combination of Reed-Solomon (RS) and convolutional codes. RS coding provides resilience against burst errors by adding parity symbols, while convolutional coding is effective for correcting random bit errors. A puncturing scheme is applied to achieve higher code rates when needed. Interleaving is then performed to scatter adjacent bits across the transmission, further mitigating the effects of burst errors.

The coded and interleaved bits are mapped to modulation symbols using different schemes, including BPSK, QPSK, 16-QAM, and 64-QAM, depending on the desired spectral efficiency and channel conditions. Gray coding is employed in the mapping process to minimize bit errors resulting from symbol demodulation.

A. OFDM Modulation and Signal Processing

Once symbol mapping is completed, the modulated data is processed by the OFDM modulator. An Inverse Fast Fourier Transform (IFFT) converts the frequency-domain symbols into a time-domain OFDM signal. To prevent ISI caused by multipath propagation, a cyclic prefix (CP) is appended to each OFDM symbol. This prefix acts as a guard interval, ensuring that delayed versions of the signal do not interfere with adjacent symbols.

At the receiver, the cyclic prefix is removed, and a Fast Fourier Transform (FFT) is applied to convert the received signal back to the frequency domain. Equalization and demodulation operations are performed to recover the transmitted symbols.

To address the challenges posed by multipath fading and time-varying channels, pilot-based channel estimation is implemented. Known pilot symbols are inserted at predetermined intervals within the OFDM frame. At the receiver, these pilots enable the estimation of channel gain and phase distortions, which can then be compensated to improve demodulation accuracy.

B. Simulation Models

The proposed system is evaluated under three primary scenarios using MATLAB/Simulink:

Model 1: AWGN Channel without Fading

This baseline model examines system performance in an Additive White Gaussian Noise (AWGN) channel, which represents thermal noise in practical systems. The objective is to benchmark Bit Error Rate (BER) performance under ideal conditions, without the effects of fading or mobility.

Model 2: Multipath Rayleigh Fading Channel

This model introduces a flat Rayleigh fading channel with multiple propagation paths, simulating real-world conditions where transmitted signals are subject to reflection, diffraction, and scattering. Parameters such as maximum Doppler shift and path delay are defined to mimic the time-varying nature of mobile channels. The impact of multipath fading on BER performance is analysed, and the benefits of channel estimation techniques are assessed.

Model 3: Adaptive Modulation and Channel Estimation

In this model, adaptive modulation and coding schemes are implemented. The system dynamically selects the modulation scheme (e.g., BPSK, QPSK, 16-QAM) based on real-time Signal-to-Noise Ratio (SNR) measurements. This allows the system to maximize throughput under favourable channel conditions and maintain link reliability during fading events. Channel estimation algorithms operate in parallel to further mitigate the impact of channel impairments.

D. MATLAB/Simulink Implementation

The simulation architecture leverages standard Simulink blocks for key signal processing functions, including random data generation, scrambling, channel coding, interleaving, IQ mapping, IFFT/FFT, cyclic prefix insertion, and AWGN/fading channel Modeling. The Multipath Rayleigh Fading Channel block is configured with realistic parameters such as Doppler spectrum type (e.g., Jakes model), maximum Doppler shift, path delay, and average path gain.

At the receiver, de-interleaving, convolutional decoding (using a Viterbi decoder), and RS decoding are performed to recover the original bit stream. A dedicated subsystem is used to extract pilot symbols and estimate channel parameters, which are then applied to compensate for gain and phase distortions.

Performance is evaluated using key metrics such as BER, constellation diagrams, and signal spectra. Multiple modulation schemes and coding rates are compared under varying SNR levels to assess the trade-offs between spectral efficiency and error performance.

E. Key Parameters and Assumptions

The simulation uses the following representative parameters:

- FFT sizes: 256, 512, 1024, and 2048 (depending on channel bandwidth)
- Subcarrier spacing: ~10-15 kHz
- Cyclic prefix length: 1/4 or 1/8 of the OFDM symbol duration
- Maximum Doppler shift: up to 40 Hz for typical vehicular speeds
- Channel coding rate: variable through puncturing
- Pilot insertion: every nth subcarrier in each OFDM symbol

The entire simulation environment is designed to be modular and adaptable, allowing for easy modification of system parameters to analyse different scenarios, including urban microcell, microcell, and indoor environments.

III. RESULTS AND DISCUSSION

This shows the Simulink block diagram for the 5G LTE physical layer model operating under an AWGN channel without fading. It includes the data generator, randomizer, channel encoder, modulator (IQ mapper), OFDM modulator (IFFT & cyclic prefix), AWGN block, OFDM demodulator, and receiver decoding chain as shown in Figure 1.

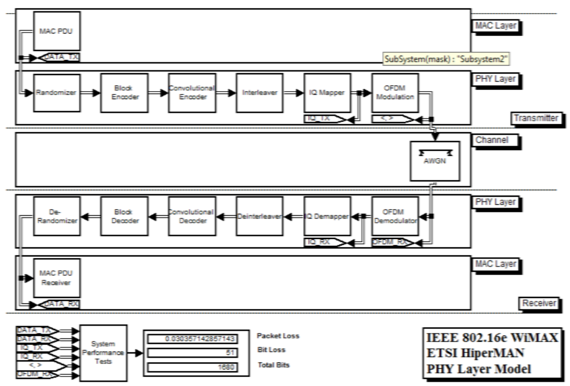

Figure 1. Simulink model of the 5G LTE physical layer under AWGN channel conditions, illustrating the baseline simulation configuration.

Figure 2, shows the 5G LTE physical layer model extended with a Multipath Rayleigh Fading Channel in addition to AWGN. It uses a multipath channel block to simulate fading effects with parameters like Doppler shift and path delays.

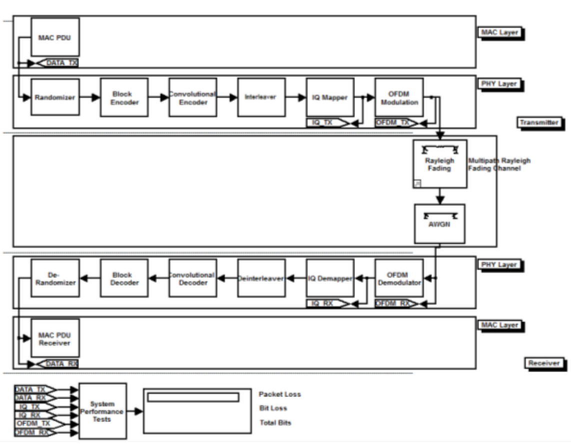

Figure 2. Simulink implementation of the 5G LTE physical layer including a Multipath Rayleigh Flat Fading Channel to emulate realistic wireless propagation conditions.

Figure 3 shows the **adaptive rate control model**, where the system uses channel estimation and pilot signals to dynamically switch modulation schemes (e.g., BPSK → QPSK → 16-QAM) depending on real-time SNR.

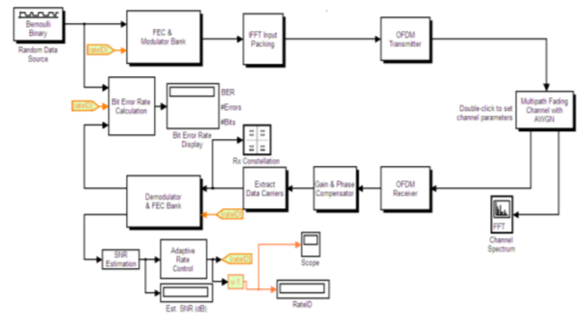

Figure 3. Adaptive modulation and channel estimation scheme for the 5G LTE physical layer, demonstrating dynamic switching between modulation levels based on estimated channel conditions.

Figure 4, A simple block diagram of the **BPSK Modulator** used for mapping binary data to phase-shifted symbols. It shows how each bit is translated into a symbol with a phase of either 0° or 180°.

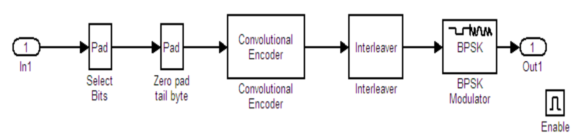

Figure 4. Block diagram of the BPSK modulator used in the 5G LTE physical layer simulation, mapping binary data to two phase states.

Figure 5, depicts the **OFDM Transmitter** subsystem, detailing the IFFT processing, subcarrier mapping, and cyclic prefix insertion that forms the composite OFDM symbol for transmission.

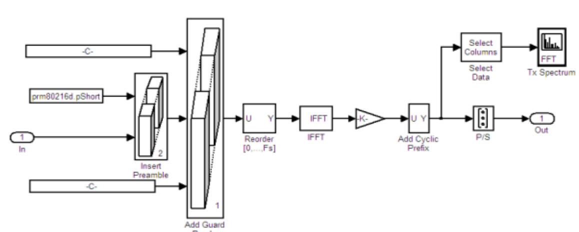

Figure 5. OFDM transmitter structure illustrating subcarrier mapping, IFFT processing, and cyclic prefix insertion for robust wireless transmission.

Figure 6, shows the OFDM **Receiver** subsystem, which performs FFT, removes cyclic prefix, and includes the channel estimation block that adjusts the received symbols before demodulation.

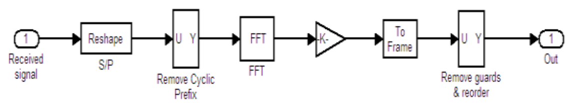

Figure 6. OFDM receiver structure highlighting cyclic prefix removal, FFT processing, and pilot-based channel estimation for signal recovery.

A. Transmit Diversity vs. Receive Diversity:

Diversity reception is a widely recognized strategy for reducing the negative impact of signal fading in wireless communication systems. Traditionally, this approach has primarily been applied at the receiver side of the communication link. However, in a notable development, Alamouti introduced a transmit diversity scheme that achieves comparable diversity benefits by employing multiple antennas at the transmitter end. This approach is particularly advantageous in practical scenarios, such as cellular networks, where equipping base stations with multiple antennas is more feasible and cost-effective than requiring each mobile device to have multiple antennas. In order to assess transmit and receive diversity, this section replicates coherent BPSK over flat-fading Rayleigh channels. Two sending and one receiving antenna (referred to as 2x1) make up the system configuration in the event of transmit diversity. On the other hand, one transmitting antenna and two receiving antennas (1x2) are used in the receive diversity arrangement. Both configurations exhibit similar computational complexity, and the simulation outcomes demonstrate that the 2x1 transmit diversity system achieves the same diversity order as the 1x2 Maximal-Ratio Combining (MRC) receive diversity system. Despite their equal diversity gains, transmit diversity experiences a performance degradation of approximately 3 dB relative to MRC. This is attributed to the assumption that the total transmitted power is kept constant in both scenarios, meaning that in transmit diversity, the power is divided between two antennas. However, if the system is adjusted so that both setups deliver the same received power, the performance of the transmit and receive diversity systems becomes equivalent. This aligns with theoretical expectations for a second-order diversity system, where total power is uniformly distributed across all available diversity branches as shown in Figure 7.

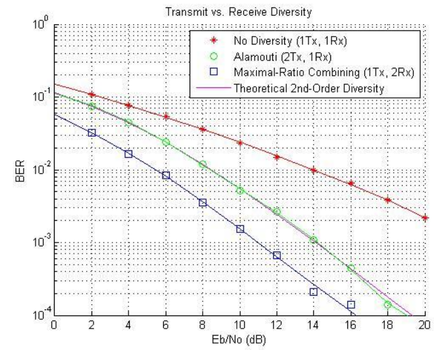

Figure 7. BER performance for 1x2 or 2x1 systems at various MIMO coding schemes.

B. Orthogonal Space-Time Block Coding and Further Explorations:

In this section, present simulation-based performance results for OSTBC using a configuration with four transmit antennas and one receive antenna, commonly referred to as a 4×1 MIMO system, implemented with a half-rate coding scheme as outlined in [4]. This setup is expected to provide a diversity order of 4, and we compare its performance against two other configurations—1×4 (one transmit and four receive antennas) and 2×2 (two transmit and two receive antennas)—which also provide the same diversity order. To ensure a fair comparison across all three configurations, we employ quaternary phase shift keying (QPSK) in conjunction with the half-rate G4 code, thereby maintaining a consistent transmission rate of 1 bit/s/Hz. Due to the computational intensity of generating these results, we utilize pre-computed data from previous simulations. The analysis is based on MATLAB scripts such as OSTBC4M.m, along with supporting files like MRC1M.m and OSTBC2M.m. These scripts serve as valuable resources for users aiming to explore and analyze other coding schemes or MIMO system configurations. The bit error rate (BER) curves for the 4×1, 2×2, and 1×4 systems show similar slopes, confirming that all three systems achieve the same diversity gain. However, the 4×1 system experiences a 3 dB degradation in performance, a result of the assumption that all systems transmit with the same total power. This loss can be mitigated by adjusting the transmit power so that each configuration delivers equal received power. When such calibration is applied, the performance of the three systems aligns closely. Moreover, the theoretical predictions correspond well with the simulated results for the 4×1 OSTBC system, provided the power is properly normalized across the diversity branches, as shown in Figure 8.

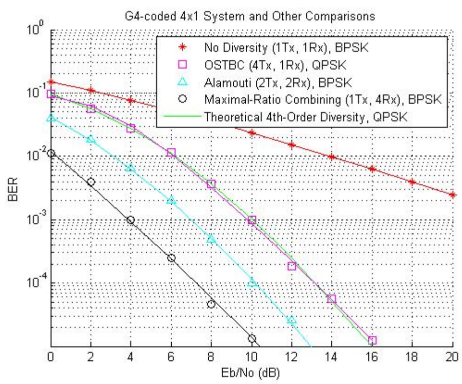

Figure 8. BER performance at different MIMO coding schemes for higher order diversity.

An adaptive algorithm has been developed to dynamically determine the appropriate modulation type and data rate based on the prevailing channel noise conditions. This algorithm begins by initializing key system parameters such as the available bandwidth, sampling factor, and guard band size, all of which influence the performance and capacity of the communication link. These parameters—bandwidth (BW), guard interval (g), and sampling frequency factor (fs)—are especially crucial in the context of MIMO-OFDM systems, where efficiency and robustness against noise and interference are critical. By evaluating the signal-to-noise ratio (SNR) and environmental variations, the algorithm selects a modulation scheme (e.g., BPSK, QPSK, QAM) and coding rate that optimize throughput while maintaining an acceptable bit error rate (BER).-

Bandwidth = max 20 Mhz
Guard band Tg = Td/8
Sampling factor fs = n.BW
After initializing the programme sampling factor is decided for the given sampling factor provide by user
fs = 22.7 Mhz
Ts = Tb + Tg

Based on parameters such as guard band size, sampling time, and available bandwidth, the algorithm determines the total data frame size, the portion allocated for useful data, and the data assigned to the guard band. It further computes the cyclic prefix index, identifying the precise address in the OFDM frame where each data symbol should be inserted prior to the application of the IFFT on the modulated symbols. Before performing the IFFT operation, the algorithm implements a series of precoding schemes to optimize signal robustness and error resilience:

- Randomization: This step involves scrambling the input data stream on a bit-by-bit basis. The goal of this process is to eliminate long sequences of identical bits (e.g., consecutive 0s or 1s) by converting them into a pseudo-random pattern. This enhances the performance of forward error correction (FEC) and modulation by improving signal characteristics and reducing spectral peaks.
- Interleaving: Interleaving rearranges the order of coded symbols over time, spreading adjacent bits apart. This mitigates the effects of burst errors by ensuring that errors introduced during transmission are distributed across multiple codewords, increasing the likelihood of successful decoding at the receiver.
- Galois Field Arithmetic: Error control coding often utilizes Galois Fields, specifically GF(2^m), to represent and manipulate data at the symbol level. This mathematical structure is fundamental in generating robust codes such as Reed–Solomon and BCH, which provide strong protection against symbol-level errors.
- Trellis Coding: This scheme applies convolutional coding and may involve puncturing, depending on the desired code rate. The number of bits removed or inserted depends on this rate, which balances redundancy and transmission efficiency.

Together, these precoding stages ensure that the transmitted data is both robust against channel impairments and optimized for high throughput, as refer Table 1.

Table 1: The algorithm chooses following modulation type and rate at different SNR.

Modulation	Coding Rate	Receiver SNR threshold (db)
BPSK	1/3	6.40
QPSK	1/3	9.40
QPSK	3/5	11.20
QAM-16	1/3	16.40
QAM-16	3/5	18.20
QAM-64	1/3	22.70
QAM-64	3/5	24.40

C. Proposed Algorithm Results:

Following a discussion and analysis of MIMO systems of data coding and transmission and OFDM performance at various modulation schemes, we will go over the results obtained for MIMO OFDM systems using the adaptive modulation strategy, which estimates the channel SNR was calculated using pilot symbols and cyclic prefix values. The program then selects the modulation scheme that would be most appropriate for minimum BER values based on the estimated SBR. The MIMO OFDM configuration that has been used is this one:

The modulation scheme options range from 1 to 5, with each option denoting:

1:Adaptive Modulation
2:BPSK
3:QPSK
4:16QAM
5:64QAM

Number of Tx antennas Mt =2, Number of Rx antennas Mr =2, Guard band ration out off total OFDM block, G=1/4, Delay spread of channel, DS =5 Number of subcarriers, L=120; Bandwidth, B=5x10^6 Hz, Signal to noise ratio is varied in dB as =[6.5 10 15 20 25 30 35 40]

The value of SNR is varied for different choice of modulation to record the effect of the noise on modulated data.

ifBPSKbitsper symbol=1
elseifOPSKbitsper symbol=2
elseif16QAMbitspersymbol=4
elseif64 QAM bitspersymbol=6

For Mt transmitters, pilot data is inserted after random binary data is created, and then the cyclix prefix is appended.A random data stream with a size of Nsym*Nfft = 6144 samples and 6 (Nsym) OFDM blocks, each with a size of 1024(Nfft), is first created. Because a cyclic prefix block was added, the transmitted signal has more length than the created block. The length of the sent signal block will be Nfft+CP since the CP length is 128. Therefore, a Tx array of size Nsym*(Nfft+CP)=6912 is initialized to store transmitted data.

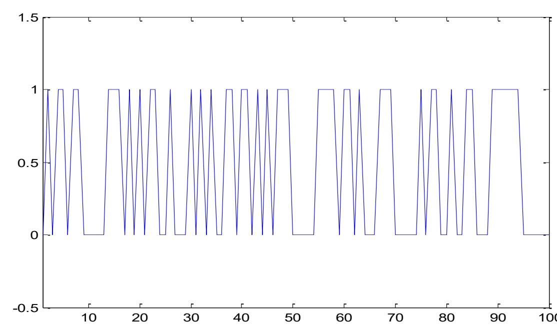

Figure 9. Initial 100 samples of generated binary data.

Following the creation of the binary data, the data is modulated. For instance, if BPSK is applied, the result is two values with the same magnitude but opposing phases, as seen in Figure 10.

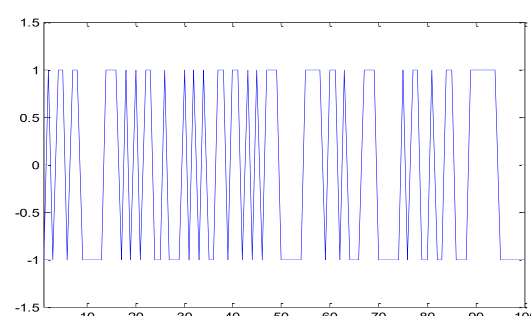

Figure 10. Initial 100 samples of BPSK modulated binary data.

The data is separated into blocks of size NFFT after the modulation is applied, and each block is subsequently subjected to ifft. The transmitted data block is created by replicating the final CP samples in the beginning of each block after applying ifft. As a result, the OFDM block matrix has a size of 1024, However, when CP is added, the Tx block has a size of 1152 samples. After adding noise to the Tx blocks at various SNR levels, a frequency offset is produced and the data array is recorded as the received block. Table 2 shows the selected parameter values for the adaptive modulation system for various SNR and bandwidth values.

Table 2 shows the selected parameter values for the adaptive modulation system for various SNR and bandwidth values.

adaptive modulation system for various SNR and The report generated by code i given below:

B.W./SNR		7	10	15	20	25
20	**Cyclic prefix**	¼	¼	**1/8**	**1/4**	**1/8**
		Modulation scheme BPSK Coding rate1/2 CPselect=193 to 256,1 to 256 CPremove=65 to 320 Input size=88 Sampling frequency=22.7	Modulation scheme QPSK Coding rate 1/2 CPselect=193 to 256, 1 to 256 CPremove=65 to 320 Input size=184 Sampling frequency=22.7	Modulation scheme QPSK Coding rate 3/4 CPselect=225 to 256,1 to 256 CPremove=33 to 288 Input size=280 Sampling frequency=22.7	Modulation scheme 16-QAM coding rate 3/4 CPselect=193 to 256, 1 to 256 CPremove= 65 to 320 Input size=568 Sampling frequency=22.7	Modulation scheme 64-QAM coding rate 3/4 CPselect=225 to 256,1 to 256 CPremove=33 to 288 Input size=856 Sampling frequency=22.7
10	**Cyclic prefix**	**1/8**	**1/8**	**1/8**	**1/8**	**1/4**
		Modulation scheme BPSK Coding rate 1/2 CPselect=225 to 256 CPremove= 33to 288 Input size=88 Sampling frequency=-11.3	Modulation scheme QPSK Coding rate 1/2 CPselect=225 to 256,1 to 256 CPremove=33 to 288 Input size=184 Sampling frequency= 11.3	Modulation scheme QPSK Coding rate 3/4 CPselect=225 to 256,1 to 256 CPremove=33 to 288 Input size=280 Sampling frequency=11.3	Modulation scheme 16-QAM Coding rate 3/4 CPselect=225 to 256,1 to 256 CPremove=33 to 288 Input size=568 Sampling frequency=11.3	Modulation scheme 64- QAM Coding rate 3/4 CPselect=193 to 256,1 to 256 CPremove=65 to 320 Input size=856 Sampling frequency=11.3
5	**Cyclic prefix**	¼	**1/8**	**1/4**	**1/4**	**1/8**
		Modulation scheme BPSK coding rate 1/2 CPselect=193 to 256,1 to 256 CPremove=65 to 320 Input size=88 Sampling frequency=5.76	Modulation scheme QPSK Coding rate 1/2 CPselect=225 to 256, 1 to 256 CPremove=33 to 288 Input size=184 Sampling frequency=5.76	Modulation scheme QPSK Coding rate 3/4 CPselect=193 to 256,1 to 256 CPremove=65 to 320 Input size=280 Sampling frequency=5.76	Modulation scheme 16-QAM Coding rate 3/4 CPselect=193 to 256,1 to 256 CPremove=65 to 320 Input size=568 Sampling frequency=5.76	Modulation scheme 64- QAM coding rate 3/4 CPselect=225 to 256,1 to 256 CPremove=33 to 288 Input size=856 Sampling frequency=5.76

bandwidth values. choose cyclic prefix to overcome delay spreads

,1/4 for longest delay spread ,1/8 for long delay spread ,
1/16 for short delay spread ,1/3 for very small delay spread channels
cSNR =6.500000000000000
Modulation scheme of BPSK with Coding rate 1/ i chosen
modscheme =Adaptive Modulation
choose cyclic prefix to overcome delay spreads
,1/4 for longest delay spread ,1/8 for long delay spread ,
1/16 for short delay spread ,1/3 for very small delay spread channels
cSNR =10
Modulation scheme of QPSK with Coding rate 1/ i chosen
modscheme =Adaptive Modulation
choose cyclic prefix to overcome delay spreads
,1/4 for longest delay spread ,1/8 for long delay spread ,
1/16 for short delay spread ,1/3 for very small delay spread channels
cSNR =15
Modulation scheme of QPSK with Coding rate 3/4 i chosen
modscheme =Adaptive Modulationchoose cyclic prefix to overcome delay spreads,1/4 for longest delay spread ,1/8 for long delay spread ,
1/16 for short delay spread ,1/3 for very small delay spread channels
cSNR = 20
Modulation scheme of 16-QAM with Coding rate 3/4 i chosen
modscheme =Adaptive Modulation
choose cyclic prefix to overcome delay spreads
,1/4 for longest delay spread ,1/8 for long delay spread ,
1/16 for short delay spread ,1/3 for very small delay spread channels
cSNR =25
Modulation scheme of 64-QAM with Coding rate 3/4 i chosen
modscheme =Adaptive Modulation
choose cyclic prefix to overcome delay spreads
,1/4 for longest delay spread ,1/8 for long delay spread ,
1/16 for short delay spread ,1/3 for very small delay spread channels
cSNR = 30
Modulation scheme of 64-QAM with Coding rate 3/4 i chosen
modscheme =Adaptive Modulation
choose cyclic prefix to overcome delay spreads
,1/4 for longest delay spread ,1/8 for long delay spread ,
1/16 for short delay spread ,1/3 for very small delay spread channels
cSNR =35
Modulation scheme of 64-QAM with Coding rate 3/4 i chosen
modscheme =Adaptive Modulation
choose cyclic prefix to overcome delay spreads
,1/4 for longest delay spread ,1/8 for long delay spread ,
1/16 for short delay spread ,1/3 for very small delay spread channels
cSNR = 40
Modulation scheme of 64-QAM with Coding rate 3/4 i chosen
modscheme =Adaptive Modulation

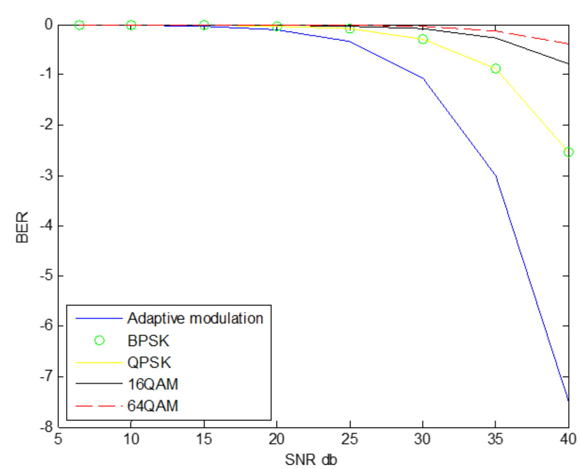

Figure 11. Performance evaluation of CP based channel estimation and correction in term of BER at different modulation for MIMO OFDM systems.

VI. CONCLUSION AND FUTURE SCOPE

This paper presents a comprehensive simulation-based evaluation of an OFDM-based 5G LTE physical layer. The analysis confirms that adaptive modulation, channel estimation, and robust coding significantly enhance performance in noisy and fading environments. Future work may include hardware implementation, power amplifier design for PAPR reduction, and integration with higher-layer protocols for full system validation.

References

[1] S. H. Han and J. H. Lee, "An Overview of Peak-to-Average Power Ratio Reduction Techniques for Multicarrier Transmission," IEEE Wireless Communications, vol. 12, no. 2, pp. 56–65, Apr. 2005.

[2] R. F. H. Fischer, "Precoding and Signal Shaping for Digital Transmission," Wiley, 2002.

[3] W. Daniel Bliss, et al., "MIMO Wireless Communications," Cambridge University Press, 2007.

[4] C. Studer, et al., "Precoding for the PAPR Reduction in Large-Scale MU-MIMO-OFDM Systems," IEEE Transactions on Signal Processing, vol. 60, no. 7, 2012.

[5] Ericsson, Ericsson Mobility Report, Datang Wireless Mobile Innovation center,2017,[Online].

[6] S. Patel, M. Chauhan, K. Kapadiya, 5G:Future mobile technology-vision 2020, J. Netw. Comput. Appl. 54(17)(2012).

[7] J. Mitola, Cognitive Radio: Model-Based Competence for Software Radios (Ph.D. Thesis), Institutionen for Teleinformatik, 1999.

[8] J. Mitola, G.Q. Maguire, Cognitive radio: making software radios more personal, IEEE Pers. Commun. 6(4) (1999)13–18.

[9] K. Kumar, A. Prakash, R. Tripathi, Spectrum handoff in cognitive radio networks: A classification and comprehensive survey, J. Netw. Comput. Appl.61(2016)161–188.

[10] A. Goldsmith, Wireless Communications, Cambridge university press, 2005.

[11] W. Liang, S.X. Ng, L. Hanzo, Cooperative overlay spectrum access in cognitive radio networks, IEEE Commun. Surv. Tutor. 19 (3) (2017) 1924–1944.

[12] M. Song, C. Xin, Y. Zhao, X. Cheng, Dynamic spectrum access: from cognitive radio to network radio, IEEE Wirel. Commun. 19 (1) (2012) 23–29.

[13] R. H. Tehrani, S. Vahid, D. Triantafyllopoulou, H. Lee, K. Moessner, Licensed Spectrum sharing schemes for mobile operators: A survey and outlook, IEEE Commun. Surv. Tutor.18(4)(2016)2591–2623.

[14] Ojha, S.; Pandey, A.K., "Close Loop V/F Control of Voltage Source Inverter using SiNUsoidal PWM, Third Harmonic Injection PWM and Space Vector PWM Method for Induction Motor." *Int. J. Power Electron. Drive Syst.* 2016, *7*, 217–224.

[15] S. Ojha, C. Sharma and A. K. Pandey, "Comparative analysis of close loop three level voltage source inverter using siNUsoidal Pulse Width Modulation and Third Harmonic Injection method for different loads," *2017 Second International Conference on Electrical, Computer and Communication Technologies (ICECCT)*, Coimbatore, India, 2017, pp. 1-6.

[16] A. P. Sinha, H. Prasad, V. K. Yadav, A. P. Singh and S. Ojha, "Navigating the EV Revolution: COVID-19's Influence and Recent Developments in EVs," *2024 1st International Conference on Innovative Sustainable Technologies for Energy, Mechatronics, and Smart Systems (ISTEMS)*, Dehradun, India, 2024, pp. 1-6.

[17] Ojha, S., & Gupta, R. (2022). Switching Frequency Formulation for Predictive Current Control in Grid-Connected VSI. IETE Journal of Research, 69(11), 8502–8510.

[18] S. Ojha and A. K. Pandey, "Comparative Analysis Of Voltage Source Inverter Using SiNUsoidal Pulse Width Modulation And Third Harmonic Injection Method For Different Levels And Loads," IJAER, vol. 10, no. 20, pp. 41451-41457, 2015.

[19] Ojha, S., & Gupta, R., "Formulation of Switching Instant for Improved Dynamic Performance in the Predictive Current Control Technique," IETE Technical Review, 40(2), 220–233.

[20] A. P. Singh, R. Gupta, S. Ojha and V. K. Yadav, "DC Bus Capacitor Discharge during Standstill and Running Condition in PMSM based EVs," *2023 11th National Power Electronics Conference (NPEC)*, Guwahati, India, 2023, pp. 1-6.

[21] Ojha S, Gupta R. Stabilization of DC-link voltage in single-phase AC/DC converter with power factor correction using predictive control algorithm. *Int J Circ Theor Appl*. 2023; 51(11): 5197-5209.
[22] A. P. Singh, R. Gupta and S. Ojha, "DC Link Voltage Balance and Discharge in Three-Level NPC Fed PMSM-Powered EVs Using External Circuit," *2024 IEEE Region 10 Symposium (TENSYMP)*, New Delhi, India, 2024, pp. 1-6.
[23] Ojha, S., Gupta, R. (2023). Selective Harmonic Compensation in Active Power Filter Using Nonlinear Predictive Current Control Method. In: Tripathi, S.M., Gonzalez-Longatt, F.M. (eds) Real-Time Simulation and Hardware-in-the-Loop Testing Using Typhoon HIL. Transactions on Computer Systems and Networks. Springer, Singapore.
[24] S. Ojha and R. Gupta, "Switching Frequency Calculation for Predictive Control Method in Active Power Filter Application," *2022 IEEE International Conference on Power* Electronics, Drives and Energy Systems, Jaipur, India, 2022, pp. 1-6.
[25] G. Sinha, S. Ojha, and A. K. Mishra, "Spectrum Utilization using Multiple Access Techniques", TIJER - INTERNATIONAL RESEARCH JOURNAL, ISSN:2349-9249, Vol.12, Issue 5, page no.b783-b789, May-2025.
[26] K. Upadhyay, S. Ojha, and A. K. Mishra, "A Comprehensive Study of Peak-to-Average Power Ratio Reduction Techniques in OFDM-Based Wireless Communication Systems," IJIRT, Vol. 12, Issue-2, pp. 1212-1220, 2025.
[27] K. Upadhyay, S. Ojha, and A. K. Mishra, "Performance Evaluation of WiMAX Physical Layer using MIMO-OFDM and Adaptive Modulation Techniques," IJIRT, Vol. 12, Issue-2, pp. 1221-1230, 2025.